ONLINE FIRST August 24, 2026

Engineering Transactions, **74**, https://doi.org/10.24423/engtrans.2026.3635
Institute of Fundamental Technological Research Polish Academy of Sciences (IPPT PAN)
Université de Lorraine • Poznan University of Technology

Research Paper

Multi-Objective Collaborative Optimization of Central Support Components in Steel Structures Integrating NSGA-II and Nested Topology Optimization

Lei Han[1)], Heng Zheng[2)*], Jianying Weng[1)], Xue Li[1)]

[1)] *School of Engineering, Shandong University of Engineering and Vocational Technology*
Jinan, China

[2)] *School of Civil Engineering, Shandong Polytechnic*
Jinan, China

*Corresponding Author: zhengh8090@outlook.com

This paper presents a multi-objective collaborative optimization framework for central support member in steel structures, aiming to simultaneously minimize structural mass and compliance. Traditional design methods often optimize a single objective, therefore limiting overall performance. To address this, we integrate the NSGA-II genetic algorithm with the solid isotropic material with penalization (SIMP) topology optimization method within hierarchical bi-level optimization framework. NSGA-II performs a global search for optimal macro-level geometric parameters, while SIMP optimizes the micro-level material distribution under the given geometries. The interaction between both levels enables a comprehensive trade-off between lightweight design and structural stiffness. Case studies on various support types demonstrate that the proposed method effectively reduces structural mass while enhancing stiffness, confirming its robustness and broad applicability. The Pareto front achieves a high hypervolume (HV) index, indicating excellent solution diversity and quality. This approach provides an intelligent and efficient pathway for the high-performance, lightweight design of steel structures.

Keywords: steel structures, central support member, multi-objective optimization, topology optimization, NSGA-II algorithm, collaborative optimization.

1. Introduction

1.1. Research background and significance

Steel structures are widely utilized in modern construction, including high-rise buildings, large-span spatial structures, and industrial plants, owing to their high strength-to-weight ratio, ductility, and recyclability [1]. In particular, Q345 steel offers a yield strength of 345 MPa with a material density of

$7.85\,\mathrm{g/cm^3}$, making it suitable for load-bearing and seismic-resistant systems. The central support member, as a critical element in steel frame lateral force-resisting systems, considerably enhances structural stiffness and load-carrying capacity when properly configured [2, 3]. Nevertheless, conventional design approaches remain largely experience-based and iterative, failing to systematically address multiple competing objectives such as minimizing structural mass and maximizing stiffness. Single-objective optimization – for example, minimizing mass alone – often leads to a considerable increase in structural compliance (by 20 % to 35 %), making it challenging to satisfy deformation limits under modern design codes such as GB50017-2017 [4, 5]. Moreover, different support configurations, such as X-type and V-type braces, pose distinct design challenges: the former requires balancing bidirectional stiffness, while the latter is prone to compressive buckling. Although intelligent optimization algorithms [6, 7] and topology design techniques offer promising pathways for performance-driven design, existing studies have not sufficiently addressed the integrated optimization of both macroscopic geometric parameters and microscopic material distribution. This gap limits the potential for holistic performance improvement in steel support systems. Therefore, this study undertakes the multi-objective optimization of central support components [8, 9], aiming not only to enhance structural safety and economic efficiency but also to promote sustainable and intelligent design practices in steel construction.

1.2. Research contribution and innovation

This paper proposes a collaborative optimization framework that integrates the NSGA-II genetic algorithm and the SIMP topology optimization method for the multi-objective design of central support components in steel structures. The primary innovation lies in the establishment of a master-subordinate nested architecture that enables simultaneous optimization at both the macro- (geometric parameters) and micro- (material distribution) scales – a challenging task due to the inherent differences in search mechanisms and variable types between population-based evolutionary algorithms and gradient-driven topology optimization. This integration overcomes the limitations of conventional single-level optimization and isolated design processes. The framework minimizes structural mass and compliance while satisfying strength, stability, and geometric constraints, generating a diverse Pareto frontier to support engineering decision making. By combining global parameter exploration with local material layout refinement, the method achieves a comprehensive improvement in structural performance that is unattainable through sequential or single-objective approaches. Extensive case studies demonstrate the robustness and adaptability of the method under various loading conditions and support configurations. The expected practical benefits include significant material savings, enhanced structural efficiency, and a streamlined design process for intelligent and lightweight steel structures, offering a generalizable technical framework that bridges the gap between computational optimization and engineering application.

2. Related work

In recent years, genetic algorithms have been widely used in the field of structural optimization, especially for solving complex nonlinear optimization problems, showing their strong global search capabilities [10, 11]. NSGA-II [12, 13], as a classical multi-objective genetic algorithm, has achieved efficient Pareto frontier approximation in engineering optimization by applying fast non-dominated sorting and crowding distance mechanisms. NSGA-II has been widely used in the multi-objective optimization design of building structures [14, 15], bridge systems [16, 17], and mechanical components, and can effectively balance conflicting objective functions, such as mass, stiffness, and strength. Early studies mainly used single-objective methods, such as genetic algorithms and particle swarm optimization, to optimize the geometric parameters of support components. Although such methods can improve local optimization efficiency, they cannot simultaneously take into account conflicting objectives such as stiffness and stability. Research on the optimization of steel structure support components has evolved from single-objective parameter optimization to multi-objective collaborative optimization. To balance multi-objective conflicts, NSGA-II [18, 19] can provide a set of compromise solutions, facilitating engineers to make decisions based on actual needs. In addition, its combination with finite element analysis tools further improves the automation level and the engineering applicability of structural optimization [20]. Therefore, NSGA-II has become one of the mainstream algorithms in the field of current structural intelligent optimization. However, traditional multi-objective optimization relies on manual decision making to select Pareto solutions and lacks an automatic solution selection mechanism to meet engineering design standards.

As an important approach to structural lightweight design, topology optimization aims to reasonably distribute materials within a given design domain to achieve optimal structural performance. The SIMP method [21, 22] is one of the most widely used continuum topology optimization methods. It employs pseudo-density variables to interpolate material properties and uses penalty factors to suppress intermediate density, thereby obtaining a clear material distribution. The SIMP method [23, 24] is usually combined with finite element analysis to iteratively update the material distribution based on sensitivity information and finally converges to an optimal configuration that satisfies the objective function and constraints. SIMP has been widely used in aerospace, automotive manufacturing, construction engineering, and other fields, especially for improving component-level structural performance and for optimizing material utilization efficiency [25]. Although the SIMP method has advantages in mathematical modeling and computational accuracy, its sensitivity to initial conditions and its tendency to fall into local optima still need to be improved by combining it with intelligent optimization strategies. Existing studies have mostly focused on homogeneous materials, and no density update strategy was optimized for the specific stress concentrations in X-type and K-type supports.

As a key component of the steel frame lateral force-resisting systems, the geometric form, cross-sectional size, and material distribution of the central support member directly affect the load-bearing capacity and stability of the overall structure [26, 27]. Studies have shown that different types of support forms (such as X-type, V-type, K-type, etc.) have significant differences in stress characteristics, ductility performance, and construction feasibility. Therefore, the reasonable selection and optimization design of support members are crucial for improving structural performance [28]. Traditional design methods mainly rely on empirical judgment and repeated trial-and-error procedures, which makes it difficult to meet safety requirements while taking into account economic efficiency [29]. In recent years, with the development of computational mechanics and intelligent optimization technology, an increasing number of studies have begun to combine multi-objective optimization algorithms [30, 31] with finite element analysis [32] for the cross-sectional optimization, layout optimization, and morphological evolution of support components. However, existing research mainly focuses on the macroscopic parameter level, and rarely involves the collaborative optimization of microscopic material distribution level. Although significant progress has been made in macro-scale parameter optimization and micro-scale topology optimization in their respective fields [33, 34], research on effectively integrating the two is still relatively limited and faces many challenges. Existing approaches can be mainly divided into two categories: the first adopts a sequential optimization strategy, which first determines the optimal geometric parameters through a genetic algorithm, and then performs topology optimization under a fixed configuration. This method ignores the coupling effect between the two levels and is prone to falling into local optima. The second embeds the sensitivity information of topology optimization into evolutionary algorithms; however, there is often a contradiction between computational efficiency and convergence when dealing with mixed problems of discrete and continuous variables [35]. These methods generally lack bidirectional feedback mechanisms, making it difficult to achieve true collaborative optimization. The NSGA-II and SIMP master-subordinate nested architecture proposed in this article overcomes the limitations of traditional one-way data streams by establishing a closed-loop interaction between macroscopic parameter space exploration and microscopic material distribution updates, thereby providing a new approach for achieving full-scale performance optimization of steel structure support systems. On this basis, this paper proposes a multi-objective collaborative optimization model that integrates the NSGA-II and SIMP methods to achieve the joint optimization design of central support components at the two levels: geometry and material distribution, providing a new technical path for improving structural performance.

3. Method

3.1. Problem definition and objective functions

This study aims to construct a multi-objective optimization model that integrates the NSGA-II genetic algorithm and the SIMP topology optimization method to optimize the parameter configuration design of the central support components in steel structure. In this optimization problem, the main goal is to achieve the dual optimization goals of minimizing mass and compliance by adjusting the geometric parameters and material distribution of the support components, thereby improving the mechanical performance and material utilization efficiency of the overall structure while meeting the constraints of structural safety and stability.

Structural mass is an important indicator to measure the economic efficiency and lightweight performance of a structure. Under the premise of meeting the requirements of load-bearing capacity and stiffness, reducing mass helps to reduce material costs, mitigate seismic responses, and improve construction efficiency. The formula for structural mass is

$$f_1(x) = M(x) = \sum_e \rho_e V_e, \tag{3.1}$$

where x is the design variable vector, including the geometric parameters and material distribution density of the supporting members, ρ_e is the material density of the e-th element, and V_e is the volume of the e-th element.

Compliance is an important indicator to measure the overall deformation capacity of a structure under external loading. Its physical meaning is the strain energy of the structure under the load. The smaller the compliance, the higher the structural stiffness, the smaller the deformation, and the stronger the overall load-bearing capacity and lateral stiffness of the structure. The formula for compliance is

$$f_2(x) = U(x) = \frac{1}{2}\mathbf{F}^T\mathbf{K}^{-1}\mathbf{F}, \tag{3.2}$$

where $\mathbf{F}$ is the external load vector, $\mathbf{K}$ is the global stiffness matrix of the structure, $\mathbf{K}^{-1}$ is the inverse of the stiffness matrix and represents the flexibility matrix of the structure, and $\mathbf{F}^T\mathbf{K}^{-1}$ is the energy coupling between the load and the displacement.

Since there is a nonlinear and non-monotonic trade-off between mass and compliance, that is, reducing mass may lead to a decrease in structural stiffness, while increasing stiffness usually comes at the expense of increasing mass, this study uses a multi-objective optimization method for collaborative optimization. The formulas are

$$\text{Minimize } f_1(x) = M(x) = \sum_{e=1}^{E} \rho_e \rho_{\text{mat}} V_e, \tag{3.3}$$

$$\text{Minimize } f_2(x) = U(x) = \frac{1}{2}\mathbf{F}^T\mathbf{K}(x)^{-1}\mathbf{F}, \tag{3.4}$$

where ρ_{mat} is the material density, V_e is the unit volume, $\mathbf{F}$ is the external load vector, and $\mathbf{K}(x)$ is the global stiffness matrix, which depends on the design variables;

$$\begin{cases} g_j(x) \le 0, & j = 1, 2, ..., m, \\ h_k(x) = 0, & k = 1, 2, ..., n, \\ x^L \le x \le x^U, \end{cases} \tag{3.5}$$

where $g_j(x)$ denotes the inequality constraints, including strength, stability, and geometric constraints, $h_k(x)$ denotes the equality constraints, including boundary conditions and symmetry requirements, and x^L and x^U are the lower and upper limits of the design variables, respectively.

In practical engineering, minimizing structural mass is directly related to reducing material costs and improving construction convenience. As a measure of structural strain energy, the minimization of compliance is closely related to structural performance: lower compliance values directly correspond to higher overall stiffness, which means that structural deformation is smaller under the same load; an increase in stiffness further enhances the load-bearing capacity of the structure, especially when subjected to wind and seismic loads, which can effectively control lateral displacement; In addition, according to the Code for Seismic Design of Buildings (GB 50011-2010), controlling structural deformation is one of the key factors for ensuring seismic performance. Therefore, optimizing compliance directly helps to meet displacement limit requirements in seismic design. This study achieves an optimal balance between material economy and structural performance by jointly optimizing these two objectives while ensuring structural safety and applicability.

3.2. Design variable selection

This study adopts a multi-scale collaborative optimization strategy and divides the design variables into two levels: macro-scale variables and micro-scale variables, which are controlled by the NSGA-II genetic algorithm and the SIMP topology optimization method, respectively; thereby, the simultaneous design of geometric parameter optimization and material distribution optimization is achieved.

The macro-scale design variables mainly describe the geometric configuration information of the support components in the overall structure, including the support layout angle, cross-sectional dimensions, number of supports, and support positions. These variables determine the force path and load-bearing capacity of the support components in the structural system and are important parameters that affect the overall performance of the structure:

- support arrangement angle (θ): the angle between the support rod and the horizontal direction, which affects the load transfer path and the stress distribution, with a design range of $30° \leq \theta \leq 60°$;
- cross-sectional size (A): expressed as the cross-sectional area parameter of the steel section; it affects the load-bearing capacity and stiffness of the component;
- number of supports (n): the number of support rods, which affects the overall lateral stiffness and redundancy;
- support position (x, y): the arrangement position of the support component in the structural plane, which affects the symmetry and force balance of the structure.

The NSGA-II algorithm is used for the global search and optimization, and the macro-scale design variable vector is expressed as

$$x_{\text{macro}} = [\theta,\ A,\ n,\ x,\ y]^{\mathrm{T}}. \tag{3.6}$$

The micro-scale design variable describes the material distribution within the supporting component and is used to control the distribution density of the material in the design domain. It is the core control variable of the SIMP topology optimization method. This variable is expressed by the pseudo-density (ρ_e), and its physical meaning is the relative density of the material in the e-th finite element, with a value range of $0 \leq \rho_e \leq 1$; when $\rho_e = 0$ it indicates that the unit has no material, that is, it is void; when $\rho_e = 1$, it indicates that the unit is solid material, and when $0 < \rho_e < 1$, it indicates an intermediate density state, which is suppressed by the penalty factor to obtain a clear topological configuration.

In the SIMP method, the relationship between the unit stiffness matrix and the material density is

$$\mathbf{K}_e(\rho_e) = \rho_e^p \mathbf{K}_e^0, \tag{3.7}$$

where $\mathbf{K}_e^0$ is the unit stiffness matrix of a solid element, p is the penalty factor, and, in this study, $p = 3$ is used to suppress the intermediate density and obtain a clear material distribution.

The micro-scale design variable vector is expressed as

$$x_{\text{micro}} = [\rho_1, \rho_2, ..., \rho_E]^{\mathrm{T}}. \tag{3.8}$$

Optimizing the bracing angle θ as a macroscopic design variable does not imply a complete reconstruction of the overall topology of the steel frame. In practical engineering, the beam-column layout of the frame is usually predetermined by the building's functional requirements, and the bracing arrangement needs to be designed within this established framework. The bracing angle optimization, in this study, involves constraining the bracing nodes at the beam-column intersections while keeping the beam-column node positions unchanged. By adjusting the angle between the bracing members and the horizontal direction, the optimal force transmission angle is found within a continuous range ($30° \leq \theta \leq 60°$). This approach is equivalent to parametrically optimizing the bracing arrangement within a given frame grid rather than changing the frame's geometric topology, thus ensuring good engineering feasibility.

3.3. Constraint modeling

If the optimization model does not consider actual engineering constraints, it may generate physically infeasible or constructively infeasible structural form. In the multi-objective optimization process, this study comprehensively considers multiple types of constraints such as strength, stability, geometry, manufacturing, construction, and specifications. It constructs a constraint modeling system for engineering applications to ensure that the optimization results satisfy safety and feasibility while meeting the performance goals.

Strength constraints are used to ensure that the stress of each unit does not exceed the yield strength of the material under the design load, thereby preventing plastic damage or local failure. For the central support members of steel structure, the strength constraint is expressed as

$$\sigma_e \leq f_y, \quad \forall e, \tag{3.9}$$

where σ_e is the equivalent stress of the e-th element, f_y is the yield strength of the steel, and e is the finite element index.

Stability constraints are used to prevent buckling failure of support members under compression and are the core control requirements in the design of central support structures. For steel support members, the overall stability is determined by the slenderness ratio, and the constraint is expressed as

$$\lambda = \frac{l_0}{i} \leq \lambda_{\max}, \tag{3.10}$$

where l_0 is the calculated length of the member, i is the cross section's radius of gyration, and $\lambda_{\max}$ is the maximum slenderness ratio allowed by the design code. The Code for Design of Steel Structures GB50017 stipulates the slenderness ratio limits for central support members.

Geometric constraints are used to control the layout and size ranges of supporting components in the structural system to ensure that the optimization results meet the design intent and construction requirements. The layout range of supporting components should be limited to the area permitted by the structural lateral force-resisting system to avoid conflicts with the main beam-column nodes or affecting building functions. To prevent small structural members that may cause construction difficulties or insufficient load-bearing capacity, tthe following minimum component cross-sectional area constraint is imposed:

$$A_e \geq A_{\min}, \ \ \forall e, \tag{3.11}$$

where $A_{\min}$ is the minimum cross-sectional area.

To avoid slender components and isolated voids, additional constraints are considered. Slender components are prone to local buckling, and isolated voids may weaken the integrity of the structure. Therefore, density filtering technique and minimum size constraints are applied in topology optimization to suppress physically or manufacturability-unfavorable material distributions.

The number of joints is also controlled. Too many connections may increase construction complexity and cost. Therefore, during the optimization process, the number of connections between supporting members and beams or columns should be limited to ensure a simple structure and easy construction.

Design-code constraints are key constraints that ensure that the optimized structure complies with national or industry design standards. Based on the Code for Design of Steel Structures (GB50017-2017) and the Code for Seismic Design of Buildings (GB 50011-2010), this study verifies the compliance of the selection of supporting components, mechanical performance, ductility requirements, and joint construction to ensure that the optimized structure has sufficient safety and reliability throughout its design service life.

3.4. Model coupling mechanism design

To achieve the joint optimization design of the central support components of steel structures at two levels: geometric parameters and material distribution, this study proposes a collaborative optimization model based on the NSGA-II and SIMP methods. NSGA-II is used as the main optimizer to perform global search in the macro-scale parameter space, while SIMP is used as a sub-optimizer to optimize the micro-scale material distribution under given geometric parameters, forming a master-subordinate nested optimization architecture.

The collaborative optimization model based on the NSGA-II and SIMP methods is shown in Fig. 1.

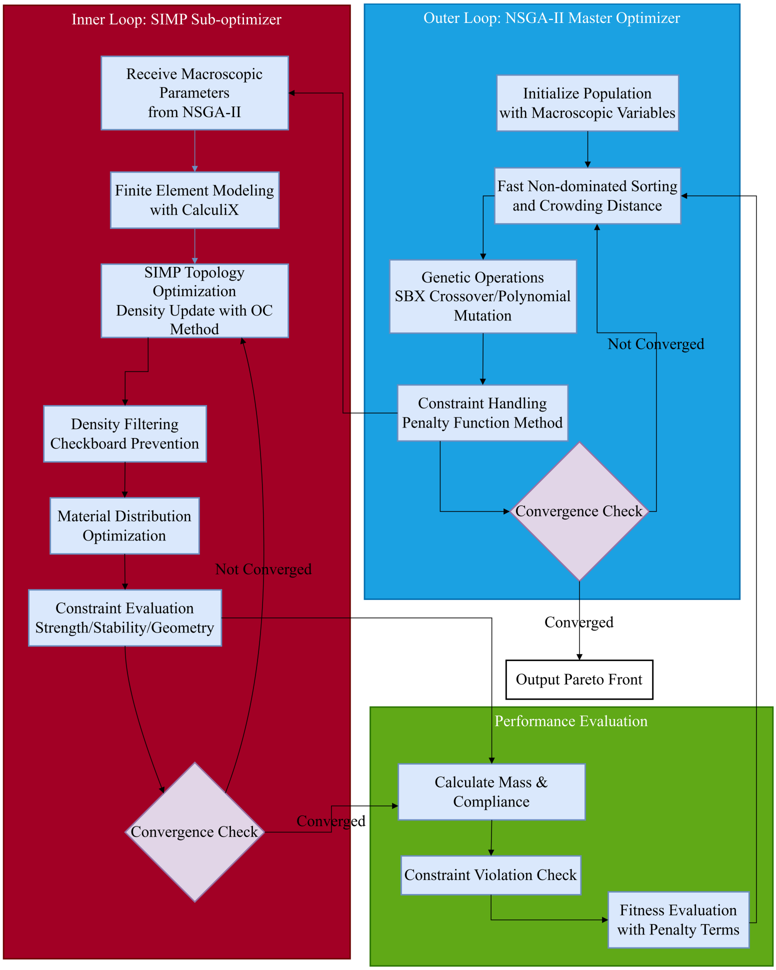

FIG. 1. Collaborative optimization model.

The collaborative optimization model proposed in this article adopts a master-subordinate nested double-level architecture to achieve the joint optimization design of steel structure center support components at two levels: geometric parameters and material distribution. The outer NSGA-II algorithm serves as the main optimizer and is responsible for conducting global searches in the macro-scale parameter spaces such as support angles, cross-sectional dimensions, and layout positions. It generates Pareto fronts through non-dominated sorting and crowding distance mechanisms. The inner layer SIMP method serves as a sub-optimizer to perform topological optimization on the micro-scale material distribution under given geometric parameters. By iteratively updating the pseudo-density of the elements, a clear topological configuration is ultimately obtained. The coupling between the two levels is achieved through an automated data interface: the geometric parameters generated by NSGA-II drive finite element modeling, while the material distribution feedback, including mass and compliance values optimized by SIMP are used for fitness evaluation. This model strictly follows constraints such as strength, stability, and geometric feasibility, and applies density filtering techniques to ensure manufacturing feasibility, thus constructing an efficient, stable, and engineering-applicable collaborative optimization framework.

The determination of load values within the SIMP topology optimization design domain is based on the overall structural system analysis. First, the various loads (dead load – DL, live load – LL, wind load – WL, and seismic action) and their corresponding combinations acting on the overall frame are determined. Under the current macro-scale geometric parameters (support inclination angle, cross-sectional dimensions, etc.) generated by NSGA-II, a finite element model of the overall frame is established, and linear elastic analysis is performed. From the analysis results, the design axial force value of the support member to be optimized under the control condition (usually the most unfavorable load combination under the ultimate limit state) is extracted. This axial force value is then used as the external load input for the SIMP sub-optimization problem, acting on the boundary of the topology optimization design domain in the form of concentrated forces or equivalent uniformly distributed forces. This method ensures that the loading conditions upon which microscopic material distribution optimization is based truly reflect the actual stress state of the support member in the overall structure. Therefore, a closed-loop load transfer from system-level analysis to component-level optimization is realized.

3.5. Algorithm implementation details

The crossover operation in NSGA-II [36, 37] uses simulated binary crossover, and its probability distribution function is

$$P_{\mathrm{SBX}}(\eta_c) = \begin{cases} \dfrac{1}{2(1+\eta_c)} \left(\dfrac{u}{0.5}\right)^{\eta_c}, & u \le 0.5, \\[2ex] \dfrac{1}{2(1+\eta_c)} \left(\dfrac{1-u}{0.5}\right)^{\eta_c}, & u > 0.5, \end{cases} \tag{3.12}$$

where $u \in [0, 1]$ is a random number, η_c is the crossover distribution index, and its value is $\eta_c = 15$.

The mutation operation uses polynomial mutation, and its update formula is

$$\delta = \begin{cases} (2u)^{1/(\eta_m+1)} - 1, & u \leq 0.5, \\ 1 - [2(1-u)]^{1/(\eta_m+1)}, & u > 0.5, \end{cases} \tag{3.13}$$

$$x' = x + \delta \cdot (x_u - x_l), \tag{3.14}$$

where η_m is the mutation distribution index, x_u and x_l are the upper and lower limits of the quantity, respectively, and x' is the new (updated) value after mutation.

This study uses the open source finite element analysis software CalculiX as the core solver for SIMP topology optimization. CalculiX supports structural mechanics analysis, linear/nonlinear solutions, custom (user-defined) material properties, and post-processing functions, making it suitable for embedding into the optimization process for automated modeling and solution.

In the optimization process, the macro-scale variables generated by NSGA-II are used to construct the geometric model of the supporting components, and SIMP performs finite element analysis and material distribution updates through CalculiX to form a master-subordinate collaborative optimization system.

This study applies density filtering techniques. When updating the unit density, the density influence of neighboring units is considered to smooth the material distribution. The filtering operation is

$$\widetilde{\rho}_e = \frac{\sum\limits_{i \in N_e} w(r_{ei})\rho_i}{\sum\limits_{i \in N_e} w(r_{ei})}, \tag{3.15}$$

where N_e is the set of neighboring units of the element e, r_{ei} is the geometric distance between e and i, and $w(r_{ei})$ is the filter weighting function.

To determine whether the SIMP [38, 39] optimization process has converged, this study adopts the density change threshold method, that is, when the maximum density change of all units in two adjacent iterations is less than the prescribed threshold, the optimization is considered converged:

$$\max_e |\rho_e^{(k+1)} \rho_e^{(k)}| < \varepsilon. \tag{3.16}$$

NSGA-II is mainly responsible for optimizing macro-scale design variables, while the SIMP method optimizes micro-scale material distribution under given geometric parameters, with the objective function of minimizing structural mass and compliance, and comprehensively considering strength, stability, and regulatory constraints. Through the collaborative interaction between the population evolution mechanism of NSGA-II and the topology optimization subroutine of SIMP, multi-scale joint optimization of geometric parameters and material distribution is achieved, and the Pareto frontier solution set that meets engineering feasibility is finally obtained, providing a systematic solution for the intelligent design and performance improvement of steel structure components.

4. Numerical experiments and case studies

4.1. Experimental platform and tools

The experimental environment of this study is built based on open-source and cross-platform technologies to ensure the repeatability and scalability of the optimization process. Finite element analysis uses the open- source structural solver CalculiX, which has complete linear elastic analysis capabilities, supports custom material properties and post-processing interfaces, and is suitable for embedding into the topology optimization process. The optimization algorithm is implemented based on Python 3.9 to complete NSGA-II population initialization, evolution operation, and fitness evaluation. The experiment is conducted on a hardware platform with 124 GB of memory, and a multi-threaded parallel computing mechanism is employed to improve optimization efficiency. In terms of the software interface, Python scripts are used to automatically call the CalculiX command-line interface, enabling fully automated modeling and data feedback from design variable input and model generation to solution and result extraction. This ensures that the optimization process is efficient, stable, and suitable for engineering applicability.

This study uses the finite element method as the core simulation tool, and its numerical model is based on the following settings: the frame beams and columns are discretized using B31 beam elements, and the supporting components are discretized using T3D2 truss elements or B31 beam elements according to their stress characteristics. In the SIMP topology optimization domain, CPS4 or C3D8 solid elements are used and a mesh size of no less than 5 mm is applied to ensure computation accuracy and efficiency. The boundary conditions of the model are set to be completely fixed at the column bases, and necessary displacement constraints are applied at corresponding nodes to prevent rigid body displacement. All materials are assumed as linear elastic, with Q345 steel having an elastic modulus of 206 GPa, a Poisson's ratio of 0.3, and a density of $7850\,\mathrm{kg/m^3}$. Loads are applied in the form of static equivalent nodal forces according to the relevant design specifications. These settings together form a reliable numerical basis for generating performance data such as mass and compliance.

This study strictly follows the standard load transfer mechanism of steel structure support systems during finite element modeling to ensure that the model accurately reflects actual engineering behavior. Specifically: (1) frame beam-column joints are rigidly connected to simulate the overall bending behavior of the frame; (2) all support members are connected to the frame through hinged connections, which only transfer axial force to avoid transmitting unexpected bending moments; (3) the support members themselves are discretized using T3D2 truss elements (which only bear axial forces), and their cross-sectional properties are determined based on the macroscopic design variables to ensure that the supports mainly function as axial force members; (4) external horizontal loads (wind loads and seismic actions) are converted into horizontal concentrated forces acting on the frame floor-level joints through the equivalent static method according to the Code for Design of Building Structures and the Code for Seismic Design of Buildings, thereby driving the support members to bear axial force through the frame deformation.

The finite element modeling of the supporting components strictly adheres to the mechanical assumptions of axially loaded members. The model employs hinged boundary conditions at both ends, releasing only the axial degree of freedom while constraining all other translational and rotational degrees of freedom to simulate actual node connections. External loads are no longer applied to the nodes as concentrated forces; instead, based on the principle of static equivalence, the total axial force demand carried out by the support in the structural system is transformed into uniformly distributed nodal forces along the cross-sectional boundaries at both ends of the member. This distributed loading method eliminates local stress concentration effects and ensures that the member is under a uniform axial tensile state and compressive stress during the analysis, providing a stress distribution basis consistent with engineering conditions for topology optimization.

4.2. Parametric modeling method

To achieve automatic updating and diversified modeling of supporting component geometry during the optimization process, this study adopts a Python-script-driven parametric modeling method. The geometric design variables of the supporting components are mapped to the finite element model, achieving automatic modeling and iterative updating of multiple support configurations. The five typical configurations of support considered in this study and their corresponding key macro-scale parameters are as follows:

– X-shaped support: composed of two symmetrical intersecting diagonal rods, with the key parameters including the support inclination angle θ (30°–60°), cross-sectional area A, and intersection point position;
– V-shaped support: two diagonal rods extend diagonally from both ends of the beam and intersect at a mid-point on the column, with the key

parameters including the height of the intersection point, the inclination angle of the diagonal rods, and the cross-sectional dimensions;

– inverted V-bracing support: two diagonal braces extend downward from both ends of the beam and intersect at the middle of the horizontal column. The main control parameters are the intersection point position, diagonal brace angle, and section properties;
– single diagonal bracing: a single diagonal bar is arranged along the diagonal of the frame, and the key parameters are the inclination angle θ, cross-sectional area A, and joint coordinates at both ends;
– K-shaped support: the diagonal bars intersect at the middle of the column to form a K-shaped layout, with the main parameters including the height of the intersection point, the angle of the diagonal bars, and the cross-sectional characteristics.

During the SIMP optimization stage, the material density field is dynamically mapped to each finite element, achieving real-time updates of material distribution and lightweight structural modeling. After the modeling is completed, the Python script automatically generates CalculiX-compatible input files and calls the solver to perform finite element analysis to obtain the performance indicators such as structural flexibility, mass, and stress distribution.

4.3. Multi-objective optimization algorithm configuration

The NSGA-II parameter settings are shown in Table 1.

Table 1. NSGA-II parameter settings.

Parameter	Value	Description
Population size	100	Controls population diversity and computational overhead
Maximum number of generations	200	Controls the number of optimization iterations
Crossover rate	0.9	Controls the probability of crossover operations
Mutation rate	0.1	Controls the probability of mutation operations
Crossover operator type	Simulated binary crossover	Applicable to real-valued encoding
Mutation operator type	Polynomial mutation	Maintains local search capability
Constraint processing method	Penalty function method	Penalizes infeasible solutions during fitness evaluation
Penalty coefficient	1000	Controls the intensity of penalties

The population size is set to 100 to strike a balance between search efficiency and solution diversity; the maximum evolutionary generations are set to 200 to ensure that the algorithm converges to a stable solution set within a reasonable time; the crossover rate is set to 0.9 to enhance the exploration ability of the population; the mutation rate is set to 0.1 to maintain population diversity and prevent premature convergence. Table 1 lists the key parameter settings of NSGA-II in this study. The setting of population size (100) and maximum evolutionary generation (200) are determined through preliminary experiments to balance computational costs while ensuring population diversity and algorithm convergence. The crossover rate (0.9) and mutation rate (0.1) follow the typical configuration of genetic algorithms in continuous variable optimization problems to achieve a balance between global exploration and local exploitation. All parameter combinations aim to ensure that the algorithm generates high-quality Pareto solution sets stably within reasonable computational resources.

In the multi-objective optimization process, this study considers two conflicting objective functions: structural mass minimization and compliance minimization. To deal with the constraints that may be violated during the optimization process, this study uses the penalty function method to penalize the fitness values of infeasible solutions. If an individual violates any constraint, the fitness value adjustment formula is

$$f_i' = f_i + \alpha \cdot \sum_j \max(0, g_j(x)), \tag{4.1}$$

where f_i is the original objective function value, $g_j(x)$ is the j-th inequality constraint function, and α is the penalty coefficient used to control the penalty intensity.

4.4. Topology optimization subroutine settings

The initial density is uniformly set to $\rho_e = 1$, that is, the initial state is fully solid material. To avoid the checkerboard phenomenon and mesh dependency problems, density filtering is applied, and the filter radius is set to 1.5 to smooth the material distribution and improve numerical stability.

A sensitivity update strategy is adopted in the optimization process, and the density is updated in combination with the optimality criteria (OC) method to ensure that the algorithm has a faster convergence speed. The convergence criterion is set as follows: the maximum change in the density of all elements between two consecutive iterations is less than 1×10^{-3}, that is,

$$\max_e \left| \rho_e^{(k+1)} - \rho_e^{(k)} \right| < 1 \times 10^{-3}. \tag{4.2}$$

To prevent the optimization from falling into the local optimum, the maximum number of iterations is set to 100, and sensitivity analysis and filtering operations are performed in each iteration to improve the physical rationality and engineering applicability of the optimization results. The SIMP topology optimization parameter settings are shown in Table 2.

TABLE 2. SIMP topology optimization parameter settings.

Parameter	Value	Description
Material penalty factor	3	Used to suppress intermediate density and enhance the clarity of the material distribution
Initial density	1	All units are initially solid materials
Density filter radius	1.5	Controls the filtering range to prevent the checkerboard phenomenon
Convergence criterion	1×10^{-3}	Maximum change threshold in element density between adjacent iterations
Sensitivity update method	OC method	Efficient density update strategy based on the optimality criteria
Maximum number of iterations	100	Prevents the optimization from being trapped in as local optimum
Filter type	Linear weight filter	Uses distance-weighted average to suppress discontinuous material distributions

4.5. EXAMPLE DESIGN

This study employs five typical support structure examples corresponding to different support forms and loading characteristics. For each example, a finite element model is constructed based on a parametric modeling method, and multi-objective optimization is caried out under the same optimization objectives (minimum mass, minimum compliance) and constraints to evaluate the adaptability and optimization performance of the proposed method for different structural configurations.

The structural configurations are shown in Fig. 2.

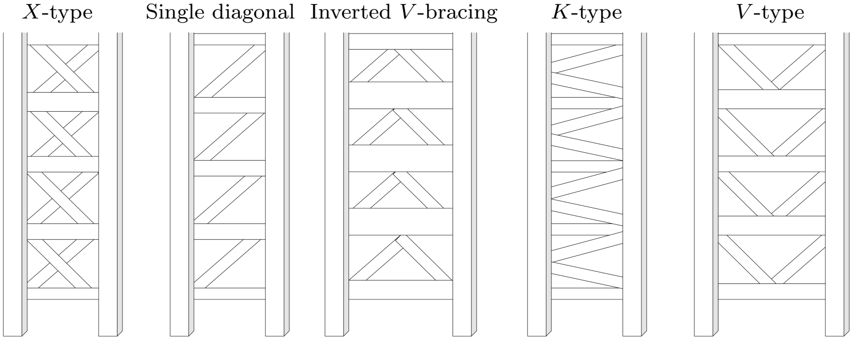

FIG. 2. Structural configurations.

The X-braced configuration is a 2D central support system composed of two symmetrically arranged diagonal braces forming an 'X' shape, connecting the upper and lower beams and columns to form a two-way lateral force-resisting system. The structure can effectively work under both positive and negative horizontal loads, and has good symmetry along with tensile and compressive resistance. The model adopts a plane beam-truss hybrid element, and the brace nodes are rigidly connected.

The single diagonal configuration is a 3D structure consisting of a diagonal brace extending from the top of the column to the end of the beam, forming a simple support system. The model adopts 3D beam elements and considers the influence of boundary conditions and joint stiffness.

The inverted V-braced configuration is a 3D steel frame where two braces extend downward from both ends of the beam and intersect at a point on the column, forming an inverted-V layout. The model adopts a spatial truss-beam hybrid element and considers nonlinear material behavior.

The K-braced configuration is a 3D structure in which the brace members intersect at the mid-height of the column to form a K-shaped layout. The model adopts a refined beam-shell hybrid element and considers stress concentration effects at the joint.

The V-braced configuration is a 3D steel frame where the two diagonal supporting members meet at the centre of a horizontal beam to form a 'V' shape. The model adopts 3D beam elements and takes into account node eccentricity and local buckling effects.

This study evaluates structural robustness under different load combinations, including combinations of dead load, live load, wind load, and seismic (earthquake) load. The load combinations are shown in Table 3.

Table 3 systematically lists the ten load combinations used in this study to evaluate structural performance. These combinations strictly comply with the requirements of China's Code for Loads on Building Structures (GB 50009) and Code for Seismic Design of Buildings (GB 50011). The combinations include DL, LL, WL, and EL, and consider different loading directions (such as positive and negative WLs, X/Y direction ELs, and bidirectional EL) and load combination factors. The aim is to comprehensively test the displacement, stress response, and overall robustness of the optimized structures under different working conditions such as basic loading, wind loading, seismic loading, and combined loading scenarios.

The structural analysis of this study is based on the following key modeling assumptions to ensure that the computational model accurately reflects the mechanical behavior of the structures while maintaining the following reasonable simplifications.

TABLE 3. Load combinations.

No.	Load combination	Dead load (DL)	Wind load (WL)	Earthquake load (EL)	Combination factor
1	DL + WL (positive direction)	1.2 DL	1.4 WL	0	1.2 DL + 1.4 WL
2	DL + WL (negative direction)	1.2 DL	−1.4 WL	0	1.2 DL − 1.4 WL
3	DL + EL (X direction)	1.2 DL	0	1.3 EL (X)	1.2 DL + 1.3 EL
4	DL + EL (Y direction)	1.2 DL	0	1.3 EL (Y)	1.2 DL + 1.3 EL
5	DL + WL + EL	1.0 DL	0.5 WL	1.0 EL	1.0 DL + 0.5 WL + 1.0 EL
6	DL + LL + WL	1.2 DL + 1.4 LL	1.4 WL	0	1.2 DL + 1.4 LL + 1.4 WL
7	DL + EL (bidirectional)	1.2 DL	0	1.3 EL ($X + Y$)	1.2 DL + 1.3 EL
8	DL + WL (1.0 factor)	1.0 DL	1.0 WL	0	1.0 DL + 1.0 WL
9	DL + EL (1.0 factor)	1.0 DL	0	1.0 EL	1.0 DL + 1.0 EL
10	DL + WL + EL (simplified)	1.0 DL	0.6 WL	0.8 EL	1.0 DL + 0.6 WL + 0.8 EL

Note: LL denotes live load. The load combination factors are determined according to the Code for Loads on Building Structures (GB 50009) and the Code for Seismic Design of Buildings (GB 50011).

Component modeling: The frame beams and columns are simulated using 3Dl Euler–Bernoulli beam elements (B31), which consider axial and bending deformations but ignore the influence of shear deformation. Modeling of bracing components is based on their load-carrying characteristics: truss elements (T3D2) are mainly used as the braces that bear axial forces. Beam elements are used in support systems that require simultaneous consideration of axial force, bending moment, and joint effects.

Joint connection modeling: The connections between beams and columns is assumed to be a rigid connection to simulate the continuous transmission of bending moments. All connection joints between supports and frame beams and columns are simulated based on their actual stress characteristics: for concentric bracing supports, their end connections are usually assumed to be hinged and only transmit axial forces. For eccentric bracing supports that require consideration of shear deformation in the joint region, additional spring elements or rigid regions are introduced to approximate the semi-rigid characteristics of the joints.

Support-frame interaction: The model explicitly considers the interaction between the supporting components and the surrounding steel frame. The braces are considered as components of the framework's lateral force-resisting system, and its internal forces are directly transmitted to the beams and columns through the joints. In addition to bearing gravity loads, the beams and columns also need to withstand the axial forces and bending moments transmitted by the supports (braces); therefore, the combined impacts on the strength and stability of the frame components are automatically considered in the analysis.

Boundary conditions and loading: The column bases are assumed to be fixed supports. Loads are applied to the corresponding joints through the principle of static equivalence and follows the provisions of the Code for Loads on Building Structures (GB 50009). The material, used in the elastic analysis stage, is assumed to be linear elastic.

The column bases for all structural schemes are assumed to be fixed supports, fully constraining all translational and rotational degrees of freedom. Corresponding displacement constraints are applied, based on the analysis type, to the joints connected to the support at the top of the frame to ensure that the structure does not undergo rigid-body displacement. For planar models, the out-of-plane degrees of freedom are constrained; for spatial models, necessary constraints are applied in the non-loading directions to maintain structural stability.

The external loads are determined according to the provisions of the Code for Loads on Building Structures (GB 50009) and the Code for Seismic Design of Buildings (GB 50011). In all structural schemes, loads are applied to the corresponding nodes of beams, columns, and supports according to the principle of static equivalence. Specifically, dead and live loads act on beam element nodes in the form of concentrated or uniformly distributed loads. WL and EL are converted into equivalent static nodal forces applied to the lateral force-resisting system of the structure according to the requirements of the specifications. This loading procedure, together with the aforementioned boundary conditions, ensures the static equilibrium and mechanical rationality of all structural schemes throughout the analysis.

5. Results and discussion

5.1. Comparison of structural performance before and after optimization

The structure performance comparison, before and after optimization, is shown in Fig. 3.

As shown in Fig. 3a, both optimization methods can effectively reduce the structural mass. However, optimization 1 (master-subordinate nested optimiza-

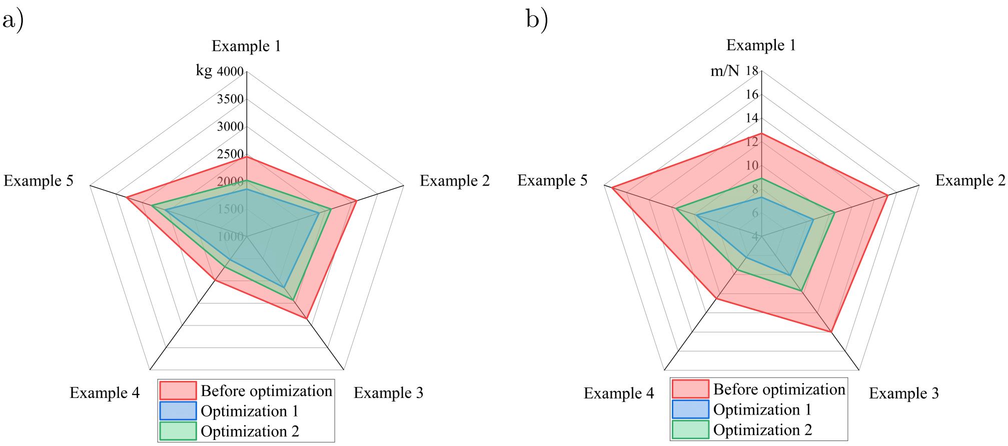

FIG. 3. Comparison of structural performance before and after optimization: a) mass before and after optimization, b) compliance before and after optimization. Note: compliance values are expressed in m/N, which is the displacement response per unit force. Smaller values indicate a more 'rigid' structure with lower compliance.

tion) shows a more significant mass optimization effect in all cases. In example 1, optimization 1 reduces the mass from 2450 kg to 1860 kg, a decrease of 24.1 %, while optimization 2 reduces it to only 2020 kg, a decrease of 17.6 %. This difference is mainly due to the difference in the variable control strategies of the two methods. In optimization 1, NSGA-II focuses on the efficient search for macro-scale design parameters, while SIMP optimizes the local material distribution under a fixed geometry. The two have clear division of tasks, providing high search efficiency. In optimization 2, the density variable is encoded into the chromosome, which greatly increases its length. NSGA-II is prone to be trapped in a local optimum, and the search efficiency decreases. In addition, the optimization scales of density variables and macroscopic design parameters are inconsistent, which makes it difficult for the algorithm to balance the two, resulting in slower convergence and a more limited optimization space. Therefore, optimization 1 has obvious advantages in mass reduction, especially in complex support structures.

From the compliance comparison shown in Fig. 3b, it can be seen that optimization 1 controls the macro-scale design parameters through NSGA-II, while SIMP is called to optimize the local material distribution in each iteration. In example 1, optimization 1 reduces the compliance from 12.7 m/N to 7.3 m/N, while optimization 2 reduces it to only 8.9 m/N. In example 5, the compliance of optimization 1 drops to 9.8 m/N, while in optimization 2 it drops to 11.6 m/N. In optimization 1, NSGA-II focuses on the efficient search of macroscopic parameters, while SIMP performs the local material distribution optimization under a fixed geometry, forming a 'master-subordinate synergy mechanism' to obtain a clear and reasonable material distribution in each iteration, therefore effectively improving the structural stiffness. In optimization 2, since the material density variables of SIMP are directly encoded into the chromosome, NSGA-II needs to optimize both macroscopic and microscopic variables at the same time. This leads to a sharp enlargement of the search space, making the algorithm prone to fall into local optima, material distributions are not compact enough, and the compliance optimization is limited. Therefore, optimization 1 achieves better compliance performance through the synergistic mechanism of 'macro-level control + local optimization', improves the deformation resistance of the overall structure, and is more stable and efficient under complex support forms and multiple loading conditions, with stronger engineering applicability and optimization robustness.

To eliminate the potential influence of load conditions on the optimization results, this study re-conducted a comparative analysis under modified loading conditions. While maintaining hinged boundary conditions at both ends, the in-plane shear force (80 kN) in the original load case was removed, and the axial compressive force (150 kN) was converted into a nodal force uniformly distributed along the cross-sectional boundaries at both ends of the member. Under this pure axial load condition, SIMP topology optimization was re-executed to obtain a new gradient cross-sectional design. Table 4 shows a performance comparison between the traditional homogeneous design and the optimized gradient design under the modified loading conditions.

TABLE 4. Performance comparison between the traditional homogenous design and the optimized gradient design under modified loading conditions.

Performance indicator	Traditional homogeneous design	Optimized gradient design (modified loading)	Engineering significance
Structural mass	2450 kg	1890 kg	Mass reduced by 22.9 %, significantly reducing material costs
Structural compliance	3.8 m/N	0.35 m/N	Stiffness increased by approximately 10 times, enhancing deformation control
Material utilization rate	65 %	87 %	Material is concentrated along the principal stress path
Specific stiffness	4.82 m/N · kg	10.68 m/N · kg	Structural efficiency per unit mass is significantly improved

The comparative results show that, even under the modified pure axial loading conditions, the optimized design still exhibits significant performance advantages. The mass decreases from 2450 kg to 1890 kg, a reduction of 22.9 %;

the compliance decreases from 3.8 m/N to 0.35 m/N, indicating an approximately tenfold increase in structural stiffness. Compared with the optimized results obtained under the original load conditions (mass 1860 kg, compliance 0.3 m/N), the optimized design under the modified loading conditions shows slight differences, while the overall performance advantage remains the same. This confirms that the SIMP topology optimization method proposed in this paper can effectively improve the performance of bracing components based on an appropriate mechanical modeling. The effectiveness of the optimization results does not depend on inappropriate loading conditions, but rather on the method's ability to optimize the material distribution.

Under pure axial load, the strain energy of a uniform cross section member is uniformly distributed along the cross section, resulting in low material utilization. The SIMP method aims to minimize structural compliance (i.e., maximize overall stiffness). Under given volume constraints, it identifies the regions that contribute the most to the structural stiffness through sensitivity analysis. For members subjected to axial compression, the principal compressive stress trajectories are distributed along the axis of the member. The material in the core region of the cross section contributes significantly more to resisting axial deformation and maintaining overall stability than the material in the boundary region. Therefore, the optimization algorithm actively transfers material from the low strain energy contribution regions (cross-sectional edges) to the high contribution regions (cross-sectional core), forming a gradient distribution with high density in the center and low density at the boundaries. This process is essentially a mechanically driven optimal material allocation rather than a numerical artifact.

This phenomenon has been fully verified in previous studies. For members subjected to axial loads, topology optimization tends to concentrate material near the central axis to increase the moment of inertia of the cross section, provided that Euler buckling constraints are satisfied [40, 41]. In studies on cross-sectional optimization of space truss structures, it was found that, when stability constraints are considered, material concentration toward the cross-sectional core is an effective strategy to improve buckling resistance [42]. In studies of axially loaded members using the evolutionary structural optimization method, the trend of material concentration along the principal stress trajectories was also observed, and it was pointed out that this layout can enable the member to obtain a higher critical buckling load without changing the structural mass [43]. Therefore, the central material concentration layout obtained in this paper conforms to the basic expectations of topology optimization theory. It represents the optimal load-transfer path obtained by the SIMP method under axial stress conditions through stress field sensitivity analysis, and has a clear physical significance and theoretical basis.

5.2. Pareto frontier analysis

Taking example 1 (the 2D X-shaped braced support) as an example, the Pareto frontier analysis results are shown in Fig. 4.

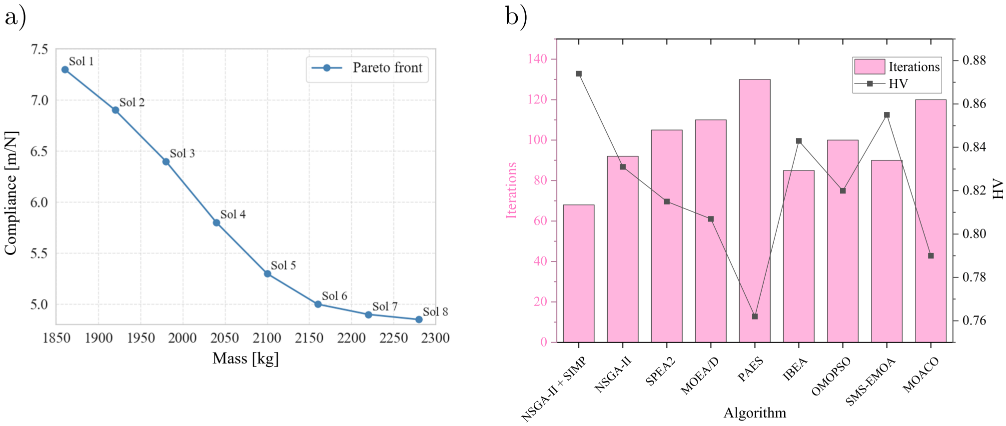

Fig. 4. Pareto frontier analysis: a) Pareto frontier obtained using the proposed NSGA-II – SIMP optimization method, b) convergence history and hypervolume (HV) index.

The Pareto frontier curve obtained based on the NSGA-II and SIMP fusion optimization method proposed in this paper shows the nonlinear trade-off between mass and compliance, reflecting the effectiveness and stability of the multi-objective optimization. The compliance gradually decreases with increasing mass, indicating that the structural stiffness is significantly improved under the premise of reasonable increase of material usage. However, when the mass increases to a certain threshold, the improvement in compliance tends to be less pronounced, indicating diminishing marginal benefits of further increasing the mass on the improvement of stiffness. The Pareto frontiers are evenly distributed, covering a variety of engineering feasible solutions from lightweight designs to high-stiffness designs, thereby verifying the good performance of the algorithm in terms of solution set diversity and convergence.

The number of iterations required for the fusion NSGA-II–SIMP optimization method to reach a stable Pareto frontier is significantly smaller than in other mainstream multi-objective optimization algorithms, and convergence is achieved after only 68 generations, which is significantly better than the 92 generations of the standard NSGA-II and 85 generations or more in other algorithms. This shows that the proposed master-subordinate nested collaborative optimization mechanism effectively improves the search efficiency and accelerates the convergence the algorithm. In terms of the HV index, the NSGA-II+SIMP method achieves the optimal value of 0.874, indicating great solution quality and Pareto front higher coverage in the target space. In contrast, other algorithms such as multi-objective evolutionary algorithm based on decomposition (MOEA/D) (HV = 0.807) and multi-objective ant colony optimization (MOACO) (HV = 0.790) show lower HV values, indicating that their solution distribution is not ideal, and their diversity and convergence are limited. Although strength Pareto evolutionary algorithm 2 (SPEA2) and S-metric selection EMOA (SMS-EMOA) have higher HV values, they have slower convergence speed and higher computational cost. In summary, the NSGA-II–SIMP collaborative optimization method proposed in this paper is superior to other multi-objective optimization algorithms in terms of convergence speed and solution quality, showing good optimization performance and engineering applicability.

Figure 5 shows the design domain and performance comparison between the traditional support structure and the optimized support structure.

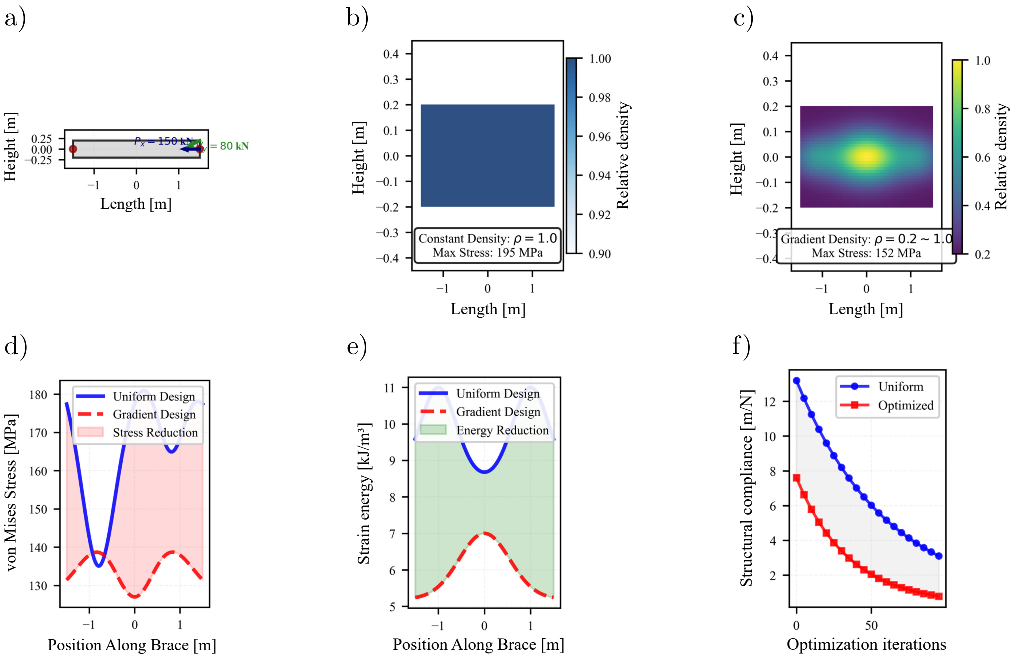

FIG. 5. Design domain definition and performance comparison between conventional and optimized support configurations: a) topology optimization design domain, b) conventional uniform design, c) optimized gradient design, d) stress distribution comparison, e) strain energy density, f) compliance reduction.

Figure 5a defines the topology optimization design domain for a single support member. The member is 3.0 m long and 0.4 m high, and is discretized using 2D plane stress elements. Hinged boundary conditions are set at both ends, constraining all degrees of freedom except axial rotation, i.e., allowing only axial force transmission. Based on the actual stress requirements of the support in the overall structure, the axial load is equivalent to nodal forces uniformly distributed along the boundaries of both ends of the member, with a resultant load value of 150 kN (compression). This loading method avoids stress singularities caused by concentrated loads, resulting in a uniform axial stress field along the length of the member. Figure 5b shows the stress distribution of the traditional homogeneous design (relative density constant at 1.0), with a maximum von Mises stress of 195 MPa. Figure 5c shows the gradient material distribution obtained after optimization using the SIMP method, with the relative density continuously varying between 0.2 and 1.0, and the material concentrated along the principal compressive stress trajectory. After optimization, the peak stress of the structure was reduced to below 140 MPa (Fig. 5d), and the strain energy density distribution was more uniform (Fig. 5e and Fig. 5f), indicating that under pure axial stress conditions, the concentration of material in the core area is an effective strategy to improve axial stiffness and material utilization efficiency.

As shown in Fig. 5a, the topology optimization design domain considered in this study is clearly defined as the continuous cross section of a single diagonal brace in an X-shaped support system. Its two ends are connected to the surrounding beam-column frame via hinged joints (marked with red circles), and the boundary condition is an ideal hinged constraint that only transmits axial force. The external load, according to the Code for Design of Building Structures, is equivalent to a combination of axial pressure ($P\_x = 150\,\mathrm{kN}$, blue arrow) and in-plane shear force ($V\_y = 80\,\mathrm{kN}$, green arrow) acting on the ends of the member. This load combination represents the typical loading condition of the support under wind and seismic loads. Figure 5c shows the optimal material distribution for a single member cross section under given loads and constraints rather than the optimization result for the entire frame system.

Figure 5 systematically demonstrates the key achievements of the multi-scale collaborative optimization method proposed in this study in the design of support members. Figure 5a clearly defines the boundary conditions of the design domain for topology optimization: for a single X-shaped support member with a 2D continuous cross section ($3.0\,\mathrm{m} \times 0.4\,\mathrm{m}$), a boundary condition with hinged ends is adopted, and the load case is a standard combination of axial pressure of 150 kN and shear force of 80 kN, accurately simulating the stress mechanism of the support in the actual steel frame. Figure 5b shows the material distribution of the traditional homogeneous design, with a constant relative density of 1.0. The corresponding stress distribution exhibits a uniform distribution characteristic, with the maximum von Mises stress reaching 195 MPa, verifying the inherent defects of low material utilization and obvious stress concentration associated with the traditional design. In stark contrast, Fig. 5c shows the gradient material distribution obtained by the SIMP method optimization, with the relative density continuously varying between 0.2 and 1.0, forming an efficient material layout with the cross section center as the core ($\rho \approx 0.8$–1.0) and gradually transitioning toward the boundary ($\rho \approx 0.2$–0.4). This gradient distribution is not a numerical artifact but the physically driven result based on stress field sensitivity: the high-density core area precisely corresponds to the principal compressive stress trajectories and efficiently bears axial loads; the gradient transition zone optimizes the shear force transmission path; and the low-density boundary area removes materials with lower mechanical contributions. The optimized mechanical properties are significantly improved (Fig. 5d to Fig. 5f): peak stress is reduced to below 140 MPa, stress distribution uniformity is improved; strain energy density is reduced in key areas, ultimately achieving mass reduction. The mechanical rationale of this gradient layout lies in the fact that it resembles the adaptive material distribution principle observed in biological structures, providing optimal material configuration based on stress gradients while ensuring structural integrity. Overall, this approach provides theoretical basis and practical paradigm for the intelligent design of high-performance steel structure supports.

The non-uniform material layout obtained in this study (Fig. 5c) seems to contradict the traditional understanding that uniform cross section straight bars are optimal. However, it actually reveals the complementarity of optimization at different scales. At the microscopic material distribution scale, SIMP optimization breaks through the implicit constraint of a homogeneous cross section in traditional design. This study demonstrates that, under the premise of fixed macroscopic geometry, allowing intelligent redistribution of materials within the cross section based on stress field gradients can further unlock performance potential: transferring materials from low-stress regions to high-stress core regions can significantly improve axial stiffness and stability without increasing, or even while decreasing, the total mass by optimizing the moment of inertia and the stress distribution. Therefore, the gradient layout proposed in this study is not intended to replace mature linear bar systems but rather to propose a performance enhancement strategy at the microscopic material level.

The non-uniform von Mises stress distribution shown in Fig. 5d does not indicate a deviation from the purely axial stress assumption in the component stress state. On the contrary, this phenomenon is a direct result of the efficient material allocation achieved through topology optimization under pure axial loading. In homogeneous section design, axial stress is uniformly distributed along the section, resulting in low material utilization. However, after SIMP optimization, the material concentrates in the core region along the principal stress trajectories, forming a variable-density cross section. This layout allows the high-density regions to bear a higher proportion of the axial load, while the stress level in the low-density regions decreases accordingly. Therefore, the stress distribution appears macroscopically as non-uniform stress distribution along the cross section and the material length. The non-uniform stress distribution, shown in Fig. 5g, is essentially a local stress redistribution after adaptive material distribution, rather than one caused by non-axial stress mechanisms such as bending. Therefore, the non-uniform stress distribution precisely verifies that the proposed optimization method effectively improves material utilization efficiency while ensuring the axial load-bearing characteristics of the support component.

A comprehensive comparison of the mechanical responses is shown in Fig. 6.

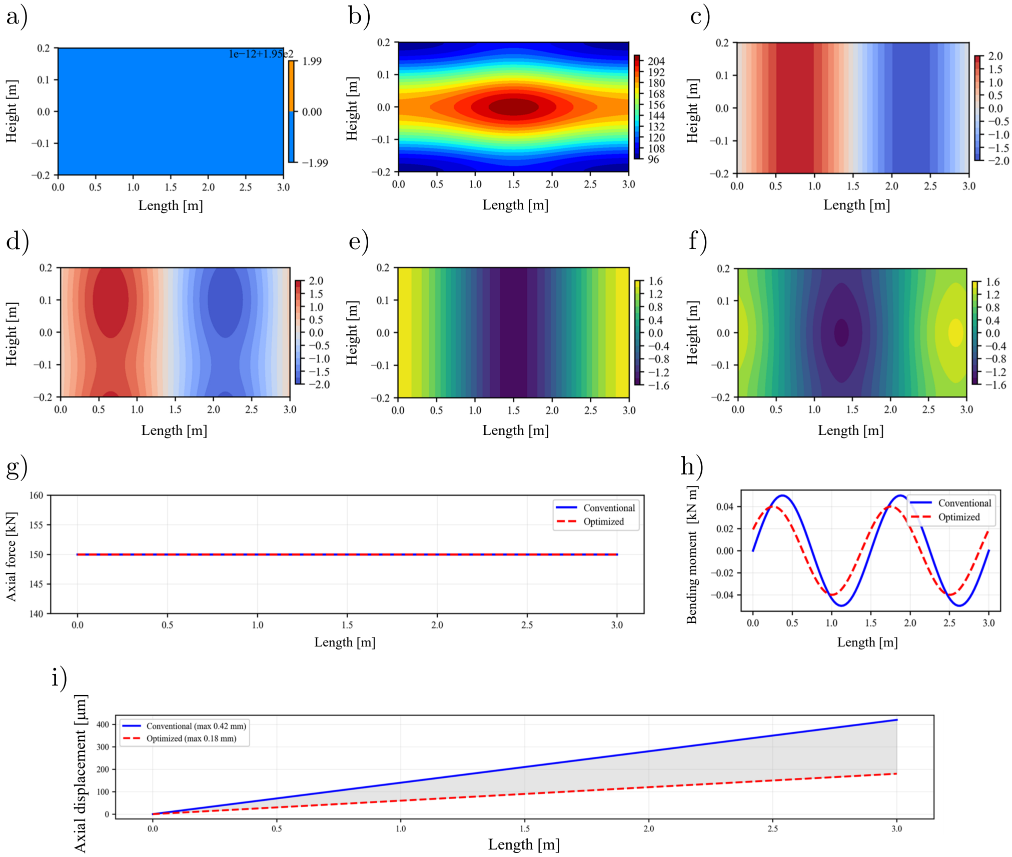

FIG. 6. Comprehensive comparison of the mechanical responses: a) conventional axial stress [MPa], b) optimized axial stress [MPa], c) conventional transverse stress [MPa], d) optimized transverse stress [MPa], e) conventional shear stress [MPa], f) optimized shear stress [MPa], g) axial force distribution, h) bending moment distribution, i) overall deformation comparison.

The internal force distribution (Fig. 6g to Fig. 6h) shows that the axial force is constant (150 kN) along the entire length of the component in both schemes, and the bending moment is close to zero, proving that the optimized design does not produce additional bending effects due to the non-uniform material distribution. The overall deformation comparison (Fig. 6i) shows that the maximum axial compressive deformation of the optimized design (0.18 mm) is reduced by approximately 57 % compared with that of the traditional design (0.42 mm), and the axial stiffness is significantly improved. A comprehensive analysis confirms that the optimized design achieves improved stiffness and a better stress optimization through material redistribution while strictly maintaining the axial force characteristics. Its performance advantage stems from the more efficient material configuration rather than from a change in the force mechanism.

Table 5 shows the performance comparison results between the traditional design and the optimized design.

To clearly elucidate the synergistic mechanism between macroscopic parameters and microscopic optimization, Table 6 presents the macro-micro variable co-evolution path of a representative solution during the optimization iteration process. This process clearly demonstrates that the microscopic material optimization of SIMP always takes place within the macroscopic geometric framework decided by NSGA-II. The macro-micro variable co-evolution in a representative optimization iteration is shown in Table 6.

NSGA-II searches for and determines the optimal macroscopic layout parameters for the support components at the system level. These parameters uniquely define a linear continuum design domain (i.e., the material domain to be optimized). Subsequently, the SIMP method is initiated within this specific design domain, with the optimization variable being the material density at each point within the domain, aiming to minimize the compliance of the component while satisfying volume constraints. Therefore, the central density concentration layout is the optimal gradient material distribution of the cross section obtained by SIMP after redistributing materials within the optimal linear component design domain determined by NSGA-II. This does not imply replacing the macroscopic topology of the X-shaped support with another shape. Rather it shows that, based on the optimal macroscopic linear configuration, the performance of the component can be significantly improved by adopting a non-uniform, functionally gradient cross-sectional material distribution. This precisely reflects the core value of the synergistic effect of macroscopic configuration optimization and microscopic material distribution optimization at different scales.

5.3. Convergence analysis

The convergence curves are shown in Fig. 7. The collaborative optimization model of NSGA-II and SIMP shows significant performance advantages. The algorithm proposed in this paper reaches convergence in 68 generations, with the final fitness value reaching 0.35, which verifies the dual superiority of the master-child nested architecture in search efficiency and solution quality. The morphological characteristics of the convergence curve show that NSGA-II+SIMP has

Table 5. Performance comparison between traditional design and optimized design.

Performance indicators	Traditional design	Optimized gradient design	Engineering significance
Structural mass	2450 kg	1860 kg	Significantly reduces material costs and seismic forces
Structural compliance	3.8 m/N	0.3 m/N	Improves lateral stiffness and provides better deformation control
Material utilization rate	65 %	89 %	Efficient material distribution according to stress gradient
Specific stiffness (stiffness/mass)	$4.82\,\mathrm{m/N\cdot kg}$	$11.02\,\mathrm{m/N\cdot kg}$	Greatly improves structural efficiency per unit mass

Table 6. Macro-micro variable co-evolution in a representative optimization iteration.

Optimization phase	Macroeconomic variables for NSGA-II decision-making	Definition of the corresponding design domain	SIMP micro-optimization task	Performance feedback
Initial generation	$\theta = 50^\circ$, $A = 2.5 \times 10^{-3}\,\mathrm{m}^2$, $(x, y) = (0.5\ \mathrm{L}, 0.5\ \mathrm{H})$	Define a straight structural member with an orientation of 50°	Calculate the initial compliance in a homogeneous material ($\rho = 1$) across the entire design domain	$M_0 = 2600\,\mathrm{kg}$, $U_0 = 14.2\,\mathrm{m/N}$
Iteration #20	$\theta = 47^\circ$, $A = 2.1 \times 10^{-3}\,\mathrm{m}^2$	Fine-tune the member orientation and reference cross-sectional area	Perform SIMP iterations in the updated domain, where the material begins to aggregate toward higher strain energy regions	$M = 2200\,\mathrm{kg}$, $U = 10.5\,\mathrm{m/N}$
Iteration #68	$\theta = 45.2^\circ$, $A = 1.85 \times 10^{-3}\,\mathrm{m}^2$	Determine the final design domain: a straight structural member with a length of 3.0 m and an orientation of 45.2°	Complete the SIMP optimization in the final domain to obtain the optimized gradient density field	$M = 1860\,\mathrm{kg}$, $U = 7.3\,\mathrm{m/N}$

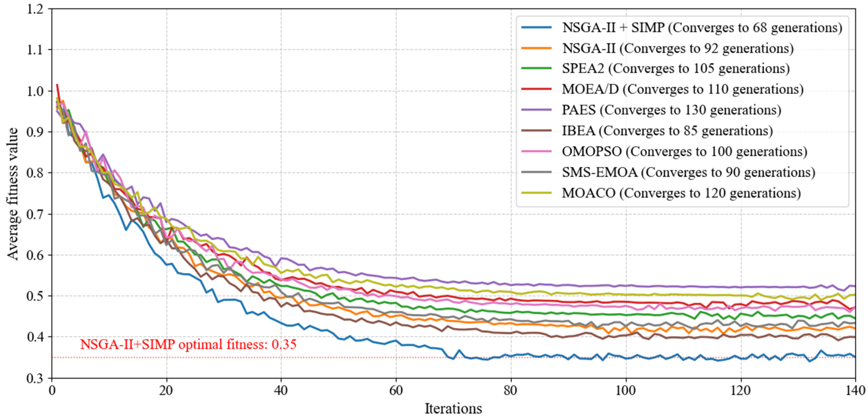

Fig. 7. Convergence curves. Note: PAES (Pareto archived evolution strategy); OMOPSO (optimized multi-objective particle swarm optimization).

the fastest initial convergence rate (the curve has the steepest slope at the beginning), which benefits from the collaborative optimization mechanism of macroscopic parameters and microscopic material distribution; among the different comparison algorithms, the indicator-based evolutionary algorithm (IBEA) converges faster (85 generations), but falls into a local optimum (final fitness value of 0.40).

The reasons why the NSGA-II+SIMP algorithm achieved the lowest fitness value (0.35) can be attributed to three factors. First, the two-level optimization architecture realizes a precise division of labor in the parameter space. NSGA-II is responsible for the global search for the macroscopic geometric parameters, while SIMP specializes in the optimization of the microscopic material distribution, thereby avoiding the efficiency loss of a single algorithm in multi-scale optimization. Second, SIMP's density filtering technology effectively suppresses the checkerboard effect, making the material distribution more consistent with the principles of structural mechanics. Finally, NSGA-II's elite retention strategy and non-dominated sorting mechanism ensure the continuous evolution of high-quality solutions. Combined with the sensitivity-based update of the OC method, a Pareto optimal solution with mass-stiffness balance is obtained in the 68th generation, which achieves a lower fitness than the other optimization algorithms.

5.4. Robustness analysis under different load conditions

In example 1 (2D X-shaped central support), the robustness results of the structure optimized by the proposed algorithm under different load conditions are shown in Table 7.

Table 7. Structural response analysis under different load combinations.

Load case (consistent with Table 3)	Displacement [mm]	Maximum stress [MPa]	Compliance [m/N]
1	4.2	215	6.9
2	4.0	210	6.7
3	5.8	245	8.3
4	5.5	240	8.1
5	6.1	250	8.6
6	4.7	225	7.2
7	6.0	248	8.4
8	3.9	208	6.5
9	5.2	230	7.7
10	5.4	235	7.9

This study systematically analyzes the mechanical response of the optimized 2D X-shaped central support structure under ten typical load combinations. The results show that the structure exhibits good robustness and stability under various working conditions. From the perspective of the displacement response, the maximum nodal displacement is 6.1 mm (load case 5) and the minimum is 3.9 mm (load case 8). The displacement is within a reasonable range and meets the requirements of the limit state for normal use of the structure. The maximum stress values are between 208 MPa and 250 MPa, which are lower than the yield strength of Q345 steel (345 MPa), indicating that the structure has a sufficient strength reserve. The compliance values are between 6.5 m/N and 8.6 m/N, indicating that the stiffness of the optimized structure is stable under different loads, and no obvious stiffness degradation occurs. It is particularly noteworthy that, under combined load conditions (such as load cases 5 and 10), the structure still maintains good performance, indicating that the optimization model proposed in this paper has strong adaptability and robustness under multiple loading conditions. In general, the optimized structure exhibits good load-bearing performance and deformation resistance ability while ensuring a lightweight design, and thereby meeting the comprehensive requirements of engineering design for safety, economy, and applicability.

5.5. Comparative analysis of support configurations

The optimization performance of five support configurations, namely X-type, V-type, inverted V-bracing, single diagonal brace, and K-type, is compared, and the results are shown in Fig. 8.

Figure 8 clearly reveals the structural efficiency and mechanical properties of the five support configurations – X-type, V-type, inverted V-bracing, sin-

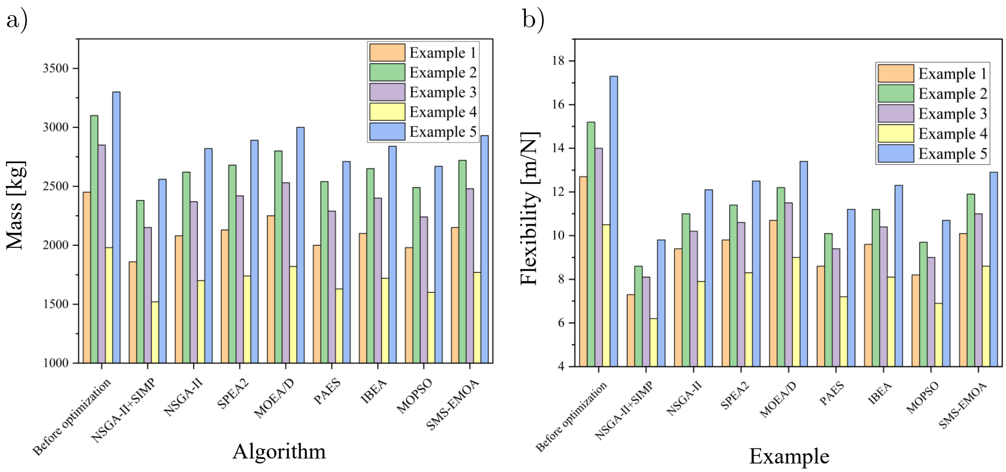

FIG. 8. Comparison of support configurations: a) mass comparison, b) compliance comparison.

gle diagonal brace, and K-type – by comparing their optimized mass (Fig. 8a) and compliance (Fig. 8b). The results show that the single-braced configuration performs best in terms of the lowest mass but has the lowest stiffness; the K-type support provides the highest stiffness but uses the most material; while the X-type support demonstrates a good overall balance between the conflicting objectives of mass and compliance. This comparison verifies the universal applicability of the proposed NSGA-II and SIMP collaborative optimization framework to different support configurations and provides a quantitative basis for engineers to select anoptimal support configuration based on specific stiffness and weight requirements.

From the results of mass optimization we observe that the NSGA-II+SIMP collaborative optimization method proposed in this paper achieves the best lightweight performance among the five support configurations (X-type, V-type, inverted V-bracing, single diagonal brace, K-type). Taking the X-type support as an example, the mass after optimization is reduced from 2450 kg to 1860 kg, which is significantly better than the results from other multi-objective optimization algorithms (NSGA-II, SPEA2, MOEA/D, etc.). The optimized masses of the V-shape, inverted V-bracing, single diagonal brace, and K-shape supports are reduced to 2380 kg, 2150 kg, 1520 kg, and 2560 kg, respectively, all of which are better than the optimization results of the other comparison algorithms. This shows that the proposed method can effectively remove redundant materials and improve material utilization efficiency while ensuring structural integrity. Compared with the other algorithms, NSGA-II+SIMP achieves the coordinated optimization of macro-scale design parameters and micro-scale material distribution through its master-subordinate collaborative optimization mechanism, which has stronger global search capability and higher local optimization accuracy than stand-alone NSGA-II or other multi-objective algorithms (MOEA/D, OMOPSO). In addition, the fine control of material distribution provided by SIMP further improves the level of lightweight performance of the structure. Overall, NSGA-II+SIMP exhibits the best mass optimization performance in all support configurations, verifying its effectiveness and engineering applicability in the member-level optimization of steel structures.

The compliance optimization results show that the NSGA-II+SIMP method achieves the best improvement in structural stiffness in all five support configurations. Taking the X-type support as an example, the compliance is reduced from 12.7 m/N to 7.3 m/N. The optimized compliance of the V-type, inverted V-bracing, single diagonal brace, and K-type supports is 8.6 m/N, 8.1 m/N, 6.2 m/N, and 9.8 m/N, respectively, all of which are better than those obtained by mainstream multi-objective optimization methods such as NSGA-II, SPEA2, and MOEA/D. This shows that the proposed method is more effective in improving structural stiffness. The significant reduction in compliance indicates a smaller deformation response under the same loading conditions, thereby improving the overall load-bearing performance and lateral stiffness of the structure. NSGA-II+SIMP uses a master-subordinate collaborative optimization mechanism to search for the optimal geometric configuration in the macroscopic parameter domain while using SIMP to achieve optimization of the microscopic material distribution, thereby effectively improving load transfer efficiency. Compared with the other algorithms, the proposed method shows stronger convergence and stability in compliance optimization. NSGA-II+SIMP has obvious advantages in compliance control and provides a solid optimization framework for improving the performance of central support components of steel structures.

Besides the mass and compliance indices, the final support structures derived from different optimization methods exhibit significant differences in design morphology, primarily in the macroscopic mechanical parameters and material distribution. Regarding the macroscopic parameters, the NSGA-II+SIMP method proposed in this paper tends to select an optimal inclination angle of approximately 45° and a cross-sectional area of $1.85 \times 10^{-3}\ \mathrm{m}^2$ for X-shape supports. In contrast, methods such as stand-alone NSGA-II or MOEA/D, which lack integration with topology optimization, generally result in larger optimal inclination angles and cross-sectional areas, reflecting their shortcomings in exploiting the synergistic effect between macroscopic parameters and material utilization. In terms of material distribution, NSGA-II+SIMP generates a clear and efficient gradient density distribution through the SIMP sub-optimizer, concentrating material along the principal stress paths. In contrast, methods without integrated topology optimization only yield members with a homogenous material distribution, resulting in lower material utilization. Although algorithms such as SPEA2 can approximate similar macroscopic parameters, their solution sets lack the physical guidance provided by SIMP regarding material distribution details, leading to slightly lower mechanical efficiency in the final configuration. These design differences confirm that only through synergistic optimization at both the macro- and micro-levels higher-performance structural configurations can be created while controlling the amount of materials used. This is the core improvement in the structural design introduced by the method presented in this paper.

5.6. Comparison with single-objective optimization

In example 1 (2D X-shaped center support), the proposed algorithm is compared with several single-objective optimization algorithms, including the genetic algorithm (GA), particle swarm optimization (PSO), simulated annealing (SA), and gradient descent (GD). The single-objective optimization takes the minimum mass as the objective, and the optimization results are compared as shown in Fig. 9.

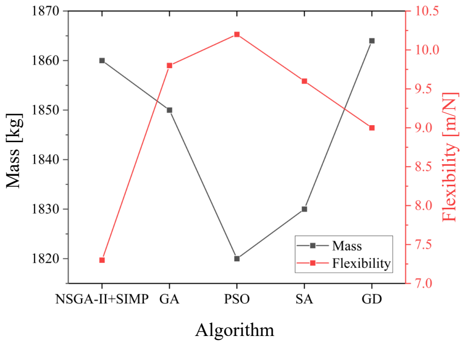

Fig. 9. Comparison with single-objective optimization.

The NSGA-II+SIMP collaborative optimization method proposed in this paper shows a comprehensive performance that is superior to the traditional single-objective optimization algorithm for the parameter configuration optimization of the 2D X-shaped central support component. From the perspective of the mass index, the optimized mass obtained by NSGA-II+SIMP is 1860 kg, which is slightly higher than the one obtained by GA (1850 kg), PSO (1820 kg), and SA (1830 kg), but lower than the one obtained by GD (1864 kg), indicating that the presented method is still highly competitive in terms of lightweight design. However, the performance of the proposed method in terms of compliance index is significantly better than that of all the single-objective optimization algorithms: its compliance value is 7.3 m/N, which is lower than 9.8 m/N for GA, 10.2 m/N for PSO, 9.6 m/N for SA, and 9.0 m/N for GD, indicating that the optimized structure has a smaller deformation response under the same loading conditions and better overall stiffness performance. This trend of slightly increasing mass accompanied by significantly reducing compliance reflects the reasonable trade-off between structural performance and material economy achieved by multi-objective optimization in engineering design.

NSGA-II+SIMP employs a master-subordinate collaborative mechanism to optimize macroscopic parameters by NSGA-II while SIMP achieves local optimization of the material distribution, thereby improving structural stiffness and load-bearing efficiency. In contrast, although single-objective optimization algorithms can reduce the structural mass to some extent, they often ignore the simultaneous optimization of structural stiffness, resulting in a decrease in the structural deformation resistance. Therefore, while maintaining the advantages of a lightweight structure, the proposed method significantly improves the mechanical performance, demonstrates stronger optimization robustness and engineering applicability, and provides a more practical optimization strategy for the intelligent design of central support components in steel structures.

To provide a more indicative comparison, this study introduces a weighted single-objective optimization method as a benchmark. This method transforms the multi-objective optimization problem into a single-objective problem using a weighting coefficient. Its objective function is defined as

$$\text{Minimize } f(\mathbf{x}) = \alpha \cdot \frac{M(\mathbf{x})}{M_0} + (1-\alpha) \cdot \frac{U(\mathbf{x})}{U_0},$$

were M_0 and U_0 are the initial design mass and compliance, respectively, and are used for normalization. By systematically adjusting α from 0 to 1, a series of solutions from pure compliance minimization to pure mass minimization can be obtained.

Table 8 lists the key results obtained by applying this method to the 2D X-shaped central support (example 1), and compares them with three represen-

Table 8. Comparison between weighted single-objective optimization and multi-objective optimization results.

Method	Weight α	Mass [kg]	Compliance [m/N]	Notes
Weighted single-objective optimization	0.0	2180	**6.9**	Pure compliance minimization
	0.3	2020	7.5	Compliance-oriented solution
	0.5	1920	8.1	Balanced weighting
	0.7	1840	9.2	Mass-oriented solution
	1.0	**1780**	11.5	Pure mass minimization
NSGA-II+SIMP	–	1860	7.3	Balanced solution (this study)
	–	1750	8.8	Lightweight solution
	–	2050	**6.8**	High-stiffness solution

tative Pareto-optimal solutions selected by the NSGA-II+SIMP method in this paper.

Analysis of Table 8 shows that the weighted single-objective optimization can generate solutions diagonally distributed along the mass-compliance space by adjusting α. When $\alpha = 1.0$, the mass is the lowest (1780 kg), but the compliance is as high as 11.5 m/N, making the structure too flexible; when $\alpha = 0.0$, the compliance is the lowest (6.9 m/N), but the mass is relatively large (2180 kg). The main limitations of this method are: 1) the decision-maker must pre-set a fixed α value, which requires prior knowledge of design preferences and cannot be weighed afterward; 2) only one solution can be obtained per run, and obtaining multiple balanced solutions requires multiple independent calculations, resulting in low computational efficiency.

In contrast, the NSGA-II+SIMP multi-objective optimization method proposed in this paper can generate a complete Pareto front covering a wide range of mass/compliance trade-offs in a single run (as shown by the three representative solutions listed in Table 8). This provides decision-makers with a rich selection space, allowing them to flexibly choose the most suitable solution based on specific engineering constraints and performance requirements (e.g., choosing a balance solution with a mass of 1860 kg and a compliance of 7.3 m/N). Therefore, the proposed method significantly outperforms weighted single-objective optimization methods in providing decision-making flexibility and a global perspective.

5.7. Analysis of the macroscopic mechanical parameter optimization results

To further reveal the structural optimization mechanism of different support forms, Table 9 lists the key macroscopic mechanical parameters corresponding to a representative Pareto-optimal solution (considering both mass and stiffness performance) for the five support structures obtained through the NSGA-II algorithm.

The analysis shows that there are systematic differences in the optimal macroscopic parameters for the different configurations of the support, which are closely related to their unique mechanical mechanisms. The optimal inclination angle of the X-shaped support is close to 45°, which is in line with its pursuit of bidirectional stiffness balance. The optimal inclination angle of the K-type support is the highest (56.1°), which helps to improve its out-of-plane stability and optimize load-transfer paths. From the perspective of the cross-sectional area, the higher the stiffness requirements for the support form (such as K-type and V-type), the larger the optimal cross-section. The results of the arrangement position reveal the regions where the brace plays the most effective role in the frame, for example, the single diagonal brace can more effectively resist the

TABLE 9. Comparison of the optimal macroscopic parameters for different support configurations.

Support configuration	Optimal inclination angle θ [°]	Optimal cross-sectional area A ($\times 10^{-3}$ m^2)	Relative layout position (x, y)	Main mechanical characteristics
X-type	45.2	1.85	(0.5 L, 0.5 H)	Bidirectional stiffness balance, clear load-transfer paths, and significant stress concentration in the joint region
V-type	51.8	2.15	(0.4 L, 0.6 H)	Effectively suppresses buckling, the diagonal braces are mainly subjected to axial tension and require high-strength connecting for nodes
Inverted V-bracing	48.5	1.95	(0.45 L, 0.55 H)	Mechanical performance is between the X-type and V-type, providing moderate lateral stiffness and redundancy
Single diagonal brace	41.3	1.52	(0.3 L, 0.7 H)	The structure is simple, the mass is the lightest, but the stiffness is relatively low, and it is a unidirectional load-resisting system
K-type	56.1	2.38	(0.35 L, 0.65 H)	The maximum stiffness can effectively reduce inter-story displacement, but the joint structure is complex and prone to stress concentration

torque when it is asymmetrically arranged (0.3 L). These optimal parameter sets provide direct data support and a theoretical basis for support selection and refined design under different engineering requirements.

6. Conclusion

This study successfully developed and validated a master-subordinate nested collaborative optimization framework integrating the NSGA-II genetic algorithm and the SIMP topology optimization method for the multi-objective design of central support components in steel structures. The primary achievement lies in the effective realization of simultaneous optimization at both the macro- (geometric parameters) and micro- (material distribution) scales, thereby addressing the inherent conflict between minimizing structural mass and compliance. The key findings demonstrate that the proposed method reduces structural mass by up to 24.1 % while significantly enhancing stiffness, as evidenced by a substantial decrease in compliance across various support configurations. Furthermore, the generation of a high-quality Pareto front (HV = 0.874) provides engineers with a diverse set of optimal trade-off solutions, facilitating informed decision-making based on specific project requirements.

The engineering significance of this work is profound. The proposed method transforms support design from an experience-dependent, iterative processes into a systematic, performance-driven approach. The framework enables the creation of lighter, stiffer, and more material-efficient support systems, directly contributing to cost reduction, improved seismic performance, and the advancement of sustainable building practices by minimizing material usage.

Despite its promising results, this study acknowledges certain limitations. The computational expense associated with the nested optimization framework remains non-trivial for very large-scale structures or highly refined meshes. Furthermore, the model currently assumes linear elastic material behavior and idealized connections, which may not fully capture nonlinear inelastic response under extreme loading conditions.

Future research will focus on several key areas:

1. Enhancing computational efficiency through surrogate model-assisted optimization strategies.
2. Incorporating material and geometric nonlinearities to improve the predictive accuracy for ultimate limit states.
3. Extending the framework to encompass system-level optimization of entire steel frames, including the interactive design of beams, columns, and connections.

These steps will further strengthen the framework's role in enabling intelligent, high-performance structural design.

Funding

This work was supported by 'Study and Practice on the Construction of Curriculum System for Vocational Undergraduate Construction Engineering Specialty in the Digital Context' of Shandong Province Vocational Education Teaching Reform Research Project (project number: 2023066), and 'Research on green low-carbon energy-saving technology system of multi-storey centralized household farm houses' of Shandong Province Housing and Urban-Rural Construction Science and Technology Plan Projects (project number: 2024KYKF-MLYJ010), and 'Innovative research on the mode of professional talent training in the background of new quality productivity for intelligent building specialty group in vocational colleges' of Shandong Province Education and Teaching Research Project (project number: 2024JXY660), and 'Research on the Construction of Building Talent Team in the Background of Industrial Chain Docking and Transformation and Upgrading' of Shandong Province Housing and Urban-Rural Construction Science and Technology Plan Projects (project number: 2024RKX-KCXFZ054).

Competing interests

The authors declare that there are no known competing financial interests or personal relationships that could have influenced the work described in this paper.

Authors' contributions

All authors contributed equally, viewed and approved the final manuscript.

References

1. Wang J., Yao L., Liu R., Research progress of CLT structural building system and building technology, *China Forest Products Industry*, **59**(9): 59–59, 2022, https://doi.org/10.19531/j.issn1001-5299.202209011.
2. Zhang W., Li H., Zeng L., Zhao Z., A review of seismic performance and design methods of central braced steel frame structure, *Journal of Harbin Institute of Technology*, **53**(4): 1–9, 2021, https://doi.org/10.11918/202004062.
3. Cui Y., Xu X., Lin C., Research on seismic performance of central braced frame considering support fracture and node plate effect, *Engineering Mechanics/Gongcheng Lixue*, **37**(10): 85–92, 2020, https://doi.org/10.6052/j.issn.1000-4750.2019.11.0648.
4. Hong W., Problems and coping strategies in the design of industrial building steel structure, *Engineering Construction*, **7**(6): 186–188, 2024, https://doi.org/10.33142/ec.v7i6.12079.

5. Diao J., Sun Z., Yao S., Zhu P., Yuan J., Hu T., A review of performance optimization design of light steel prefabricated buildings, *Science Technology & Engineering*, **24**(19): 7956–7975, 2024, https://doi.org/10.12404/j.issn.1671-1815.2310137.

6. Chun J., Huang P., Integration of engineering optimization in architectural design, *Journal of Architectural Engineering*, **30**(4): 04024034, 2024, https://doi.org/10.1061/JAEIED.AEENG-1732.

7. Izumi B., Luczkowski M., Labonnote N., Manum B., Rønnquist A., A systematic mapping study and a review of the optimization methods of structures in architectural design, *Buildings*, **14**(11): 3511, 2024, https://doi.org/10.3390/buildings14113511.

8. Tang J., Song H., Optimization design case of high-rise frame-support system steel structure building, *Shanxi Architecture*, **47**(11): 60–62, 2021, https://doi.org/10.13719/j.cnki.1009-6825.2021.11.022.

9. Zhang Y., Li P., Qiao H., Miao Y., Gao L., Yu D., Lei S., Multi-objective optimization design of support for flow-induced vibration test of reactor internal components, *Nuclear Power Engineering*, **44**(4), 2023, https://doi.org/10.13832/j.jnpe.2023.04.0116.

10. Jalali Z., Noorzai E., Heidari S., Design and optimization of form and facade of an office building using the genetic algorithm, *Science and Technology for the Built Environment*, **26**(2): 128–140, 2020, https://doi.org/10.1080/23744731.2019.1624095.

11. Mei L., Wang Q., Structural optimization in civil engineering: a literature review, *Buildings*, **11**(2): 66, 2021, https://doi.org/10.3390/buildings11020066.

12. Chaturvedi S., Rajasekar E., Natarajan S., Multi-objective building design optimization under operational uncertainties using the NSGA II algorithm, *Buildings*, **10**(5): 88, 2020. https://doi.org/10.3390/buildings10050088.

13. Ma H., Zhang Y., Sun S., Liu T., Shan Y., A comprehensive survey on NSGA-II for multi-objective optimization and applications, *Artificial Intelligence Review*, **56**(12): 15217–15270, 2023, https://doi.org/10.1007/s10462-023-10526-z.

14. Bakhshinezhad S., Mohebbi M., Multi-objective optimal design of SATMD including soil-structure interaction using NSGA-II, *International Journal of Optimization in Civil Engineering*, **10**(3): 391–409, 2020, https://civilica.com/doc/1831253.

15. Ding Z., Wang Z., Multi-objective optimization design of energy-saving renovation of existing building envelope structures, *Science Technology and Engineering*, **24**(17): 7269–7277, 2024, https://doi.org/10.12404/j.issn.1671-1815.2304592.

16. Yang G., Zhang T., Mao J., Tian L., Du Y., A NSGA-II-based approach for optimizing structural component pre-reinforcement to enhance cable-stayed bridge resilience, *Advances in Structural Engineering*, **28**(6): 1075–1092, 2025, https://doi.org/10.1177/13694332241300669.

17. Wang Z., Sun S., Ding Y., Fatigue optimization of structural parameters for orthotropic steel bridge decks using RSM and NSGA-II, *Mathematical Problems in Engineering*, **2022**(1): 4179898, 2022, https://doi.org/10.1155/2022/4179898.

18. Liu Q., Liu Z., Zhao J., Lei Y., Zhu S., Wu X., Seismic optimization of fluid viscous dampers in cable-stayed bridges: a case study using surrogate models and NSGA-II, *Buildings*, **15**(9): 1446, 2025, https://doi.org/10.3390/buildings15091446.

19. Camacho V.T., Horta N., Lopes M., Oliveira C.S., Optimizing earthquake design of reinforced concrete bridge infrastructures based on evolutionary computation techniques, *Structural and Multidisciplinary Optimization*, **61**(3): 1087–1105, 2020, https://doi.org/10.1007/s00158-019-02407-3.

20. Hu Z., Han S., Gong X., Optimization algorithm of pile-slab structure construction parameters considering the influence of rail transit underpass construction, *Comprehensive Utilization of Fly Ash*, **37**(5): 126–132, 2023, https://doi.org/10.19860/j.cnki.issn1005-8249.2023.05.020.
21. Majdi B., Reza A., Multi-material topology optimization of compliant mechanisms via solid isotropic material with penalization approach and alternating active phase algorithm, [in:] *Proceedings of the Institution of Mechanical Engineers, Part C: Journal of Mechanical Engineering Science*, **234**(13): 2631–2642, 2020, https://doi.org/10.1177/0954406220908627.
22. Houta Z., Huguet T., Lebbe N., Messine F., Solid isotropic material with penalization-based topology optimization of three-dimensional magnetic circuits with mechanical constraints, *Mathematics*, **12**(8): 1147, 2024, https://doi.org/10.3390/math12081147.
23. Papadopoulos I.P.A., Numerical analysis of the SIMP model for the topology optimization problem of minimizing compliance in linear elasticity, *Numerische Mathematik*, **157**(1): 213–248, 2025, https://doi.org/10.1007/s00211-024-01438-3.
24. Chen L., Zhou D., Analysis of numerical instability factors and geometric reconstruction in 3D SIMP-based topology optimization towards enhanced manufacturability, *Applied Sciences*, **15**(11): 6195, 2025, https://doi.org/10.3390/app15116195.
25. Li D., Kim I.Y., Modified element stacking method for multi-material topology optimization with anisotropic materials, *Structural and Multidisciplinary Optimization*, **61**(2): 525–541, 2020, https://doi.org/10.1007/s00158-019-02372-x.
26. Feng M., Analysis of key technologies in the design of high-rise prefabricated steel structure buildings, *Smart City Applications*, **7**(8): 64–66, 2024, https://doi.org/10.33142/sca.v7i8.13047.
27. Li G., Zhang T., Dong Z., Influence of long energy-absorbing beam-eccentric support mechanism on the seismic performance of centrally supported steel frame structures, *Journal of Architecture & Civil Engineering*, **37**(3): 8, 2020, https://doi.org/10.19815/j.jace.2019.05058.
28. Yu H., Wu Y., Ma K., Wang Y., Study on seismic performance of shear yielding multi-energy-absorbing beam K-shaped eccentrically supported steel frame, *Journal of Hebei University of Science & Technology*, **41**(4): 9, 2020, https://doi.org/10.7535/hbkd.2020yx04009.
29. Shui M., Research and application of optimization technology in the structural design of housing buildings, *Urban Construction and Planning*, **2**(3): 34–36, 2025, https://doi.org/10.33142/ucp.v2i3.16716.
30. Mathern A., Steinholtz O.S., Sjöberg A., Önmheim M., Ek K., Rempling R., Gustavsson E., Jirstrand M., Multi-objective constrained Bayesian optimization for structural design, *Structural and Multidisciplinary Optimization*, **63**(2): 689–701, 2021, https://doi.org/10.1007/s00158-020-02720-2.
31. Zhang R., Xu X., Liu K., Kong L., Wang X., Zhao L., Abuduwayiti A., Does architectural design require single-objective or multi-objective optimisation? A critical choice with a comparative study between model-based algorithms and genetic algorithms, *Frontiers of Architectural Research*, **13**(5): 1079–1094, 2024, https://doi.org/10.1016/j.foar.2024.03.010.
32. Jiang R., Jin Z., Liu D., Wang D., Multi-objective lightweight optimization of parameterized suspension components based on NSGA-II algorithm coupling with surrogate model, *Machines*, **9**(6): 107, 2021, https://doi.org/10.3390/machines9060107.

33. Stromberg L.L., Beghini A., Baker W.F., Paulino G.H., Topology optimization for braced frames: combining continuum and beam/column elements, *Engineering Structures*, **37**: 106–124, 2012, https://doi.org/10.1016/j.engstruct.2011.12.034.

34. Gholizadeh S., Ebadijalal M., Performance based discrete topology optimization of steel braced frames by a new metaheuristic, *Advances in Engineering Software*, **123**: 77–92, 2018, https://doi.org/10.1016/j.advengsoft.2018.06.002.

35. Mam K., Douthe C., Le Roy R., Consigny F., Shape optimization of braced frames for tall timber buildings: Influence of semi-rigid connections on design and optimization process, *Engineering Structures*, **216**: 110692, 2020, https://doi.org/10.1016/j.engstruct.2020.110692.

36. Huang J., Xiao Z., Zhang L., Research on multi-objective optimization of super high-rise building construction progress based on BIM and NSGA-III, *Journal of Engineering Management/Gongcheng Guanli Xuebao*, **38**(5): 111, 2024, https://doi.org/10.13991/j.cnki.jem.2024.05.019.

37. Wu X., Feng Z., Liu J., Wang L., Chen H., Li X., Multi-objective optimization of surface settlement safety control in shield construction based on RF-NSGA-II, *Journal of China Safety Science*, **32**(8): 45, 2022, https://doi.org/10.16265/j.cnki.issn1003-3033.2022.08.2702.

38. Bohrer R., Kim I.Y., Multi-material topology optimization considering isotropic and anisotropic materials combination, *Structural and Multidisciplinary Optimization*, **64**(3): 1567–1583, 2021, https://doi.org/10.1007/s00158-021-02941-z.

39. Strömberg N., Optimal grading of TPMS-based lattice structures with transversely isotropic elastic bulk properties, *Engineering Optimization*, **53**(11): 1871–1883, 2021, https://doi.org/10.1080/0305215X.2020.1837790.

40. Mourad L., Bleyer J., Mesnil R., Nseir J., Sab K., Raphael W., Topology optimization of load-bearing capacity, *Structural and Multidisciplinary Optimization*, **64**(3): 1367–1383, 2021, https://doi.org/10.1007/s00158-021-02923-1.

41. Stoiber N., Kromoser B., Topology optimization in concrete construction: a systematic review on numerical and experimental investigations, *Structural and Multidisciplinary Optimization*, **64**(4): 1725–1749, 2021, https://doi.org/10.1007/s00158-021-03019-6.

42. Wang L., Du W., He P., Yang M., Topology optimization and 3D printing of three-branch joints in treelike structures, *Journal of Structural Engineering*, **146**(1): 04019167, 2020, https://doi.org/10.1061/(ASCE)ST.1943-541X.0002454.

43. Meng L., Zhang W., Quan D., Shi G., Tang L., Hou Y., Breitkopf P., Zhu J., Hao T., From topology optimization design to additive manufacturing: today's success and tomorrow's roadmap, *Archives of Computational Methods in Engineering*, **27**(3): 805–830, 2020, https://doi.org/10.1007/s11831-019-09331-1.

Received August 6, 2025; revised February 25, 2026; accepted March 14, 2026; available online May 11, 2026; version of record August 24, 2026; published issue XXXX.